Switching Power System Stabilizer and Its Coordination for Enhancement of Multi-machine Power System Stability

Yang Liu, Q. H. Wu, *Fellow, IEEE*, Haotian Kang, Xiaoxin Zhou, *Fellow, CSEE, Fellow, IEEE*

***Abstract*—This paper proposes a coordinated switching power system stabilizer (SPSS) to enhance the stability of multi-machine power systems. The SPSS switches between a bang-bang power system stabilizer (BPSS) and a conventional power system stabilizer (CPSS) based on a state-dependent switching strategy. The BPSS is designed as a bang-bang constant funnel controller (BCFC). It is able to provide fast damping of rotor speed oscillations in a bang-bang manner. The closed-loop stability of the power system controlled by the SPSSs and the CPSSs is analyzed. To verify the control performance of the SPSS, simulation studies are carried out in a 4-generator 11-bus power system and the IEEE 16-generator 68-bus power system. The damping ability of the SPSS is evaluated in aspects of small-signal oscillation damping and transient stability enhancement, respectively. Meanwhile, the coordination between different SPSSs and the coordination between the SPSS and the CPSS are investigated therein.**

***Index Terms*—Bang-bang PSS, coordinated switching PSS, multi-machine power systems.**

I. Introduction

POWER system oscillations caused by load changes, renewable energy penetration, and external disturbances can lead to low-frequency and sub-synchronous oscillations of a power system. A condition that can further lead to voltage collapse, islanding, and blackouts. As such, the small-signal stability has long been regarded as a key issue in the operation of large scale multi-machine power systems, with scope for improvements realized through the application of conventional power system stabilizers (CPSSs).

The CPSS mechanism involves adding auxiliary damping to rotor speed oscillations [1]. However, CPSS has inherent defects that significantly diminish its control performance, as follows: First, the CPSS is designed based on the linearized model of a power system operating at a specific operation point. The location selection and parameter tuning of a CPSS rely on the deterministic operation point of the system, in which constant system parameters and particular load levels are assumed [2]. However, the system parameters and load levels are always changing during its normal operations and the operation point of the power system can vary based on external disturbances [3]. Second, the control performance of the CPSS is largely determined by the accuracy of system parameters based on which the CPSS is designed, whereas, in practice, absolutely accurate system parameters are rarely available [4]. Third, installed CPSSs in a large-scale power system experience complex interactions with no decoupling mechanism, which means that their coordinated control performance can subsequently be severely undermined [5].

In addition to CPSSs, considerable study has been devoted to the design of robust, probabilistic and adaptive power system stabilizer (PSS). A robust PSS was proposed in [6], in which the PSS was claimed to be robust to both the transient and small-signal oscillations of the power system based on the trajectory sensitivity of rotor speed. In fact, a specific set of PSS parameters cannot be optimal to all oscillation modes of the power system. The same problem surfaces in the probabilistic PSS proposed in [7]. Here, the expectation and variance sensitivity of the eigenvalues of a power system operating under different operation modes are evaluated to determine the PSS parameters. Moreover, a decentralized adaptive PSS was designed based on a reduced-order state observer as described in [8]. This study utilized the information of the relative rotor speed between the generators having strong interactions to generate the estimation of state variables. Moreover, the accuracy of the estimated states relied on the high gain parameters of the state observer. However, in this case, the noise of the measured signal would be magnified and seriously damage the control performance of the proposed adaptive PSS.

This paper proposes a bang-bang PSS (BPSS) based on the bang-bang funnel controller (BBFC) to achieve fast damping of small-signal oscillations of power systems. The BBFC was first proposed in [9] for nonlinear system with arbitrary known relative degree. Under BBFC feasibility assumptions, the system output tracking error and its derivatives can be regulated within pre-specific error funnels. Taking advantage of the BBFC, the BPSS is designed as a bang-bang constant funnel controller. The constant funnel values of the BPSS can significantly improve its applicability in practice, which simplifies the funnel design process.

Manuscript received October 17, 2015; revised January 2, 2016; accepted April 6, 2016. Date of publication June 30, 2016; date of current version May 20, 2016. This work was funded by State Key Program of National Natural Science of China (No. 51437006), and Guangdong Innovative Research Team Program (No. 201001N0104744201), China.

Yang Liu, Q. H. Wu (corresponding author, e-mail: wuqh@scut.edu.cn), and Haotian Kang are with the School of Electric Power Engineering, South China University of Technology, Guangzhou 510640, China.

Xiaoxin Zhou is with China Electric Power Research Institute, State Grid Corporation of China, Qinghe, Beijing 100192, China.

DOI: 10.17775/CSEEJPES.2016.00027

The main contribution of this work can be summarized as follows. First, a coordinated SPSS is designed to switch between a BPSS and a CPSS based on an appropriately designed switching strategy. Second, a two-stage, state-dependent switching strategy is proposed. If external disturbances occur in the power system, the BPSS is switched on first to regulate the rotor speed deviation and its derivatives into the pre-specified error funnels. Referring to the switching strategy of the SPSS and if specific switching condition is satisfied, the CPSS is switched on to stabilize the power system to its original operation point asymptotically. On one hand, this switching strategy makes full use of the damping ability of the CPSS near the equilibrium point. On the other hand, a faster convergence rate can be achieved by the implementation of the BPSS, which has intrinsic time-optimum characteristics during the initial post-disturbance stage. Third, the closed-loop stability of the entire power system implemented with the SPSSs and the CPSSs is analyzed. Fourth, simulation studies are undertaken in a 4-generator 11-bus power system and the IEEE 16-generator 68-bus power system to evaluate the small-signal oscillation damping performance and transient stability improvement of the SPSS, respectively. The coordination between different SPSSs and the coordination between the SPSS and the CPSS are studied therein.

In contrast to the switching excitation controller studied in [10], the SPSS is mainly dedicated to improving the small-signal stability of power systems. Although the methodologies of the SPSS and the switching excitation controller are similar, the switching excitation controller is only designed for the regulation of power systems confronting large disturbances. In instances where that small disturbances occur in a power system, the switching excitation controller will not work. Moreover, the required inputs of the SPSS and the switching excitation controller are different. The input variable of the SPSS is the rotor speed deviation of a generator, while that of the switching excitation controller is the rotor angle deviation of a generator. Furthermore, the SPSS is merely a part of the excitation system, and it only responds to the frequency deviation of generators. The SPSS also has positive effects on the transient stability of power systems, which will be evaluated in this work as well.

The SPSS does not conflict with the switching excitation controller proposed in [10]. The trigger value of the BPSS is much smaller than that of the bang-bang excitation controller, thus the switching excitation controller cannot be triggered in the cases where small disturbance occurs in power systems. When large disturbances occur, the switching excitation controller is triggered, while the SPSS installed on the same generator is blocked. The SPSSs installed on other generators are then triggered to provide damping to the oscillations caused by large disturbances.

This paper is organized as follows. The model of a multi-machine power system and its partial linearization are presented in Section II. Section III illustrates the design of the SPSS. Then the closed-loop stability of the whole system is analyzed in Section IV. Simulation studies are carried out in Section V. Finally, conclusions are presented in Section VI and appendices follow thereafter.

II. Power System Modeling

A fourth-order synchronous generator model with a first-order excitation controller taken into consideration is employed here. A n machine power system, in which the nth machine is chosen as the reference machine, can be denoted as follows [11]

$$\begin{cases} \Delta\dot{\delta}_i = \omega_{\mathrm{B}}\Delta\omega_i \\ \Delta\dot{\omega}_i = \dfrac{1}{2H_i}(P_{\mathrm{m}i} - P_{\mathrm{e}i} - D_i\Delta\omega_i) \\ \dot{E}'_{\mathrm{q}i} = \dfrac{1}{T'_{\mathrm{d}0i}}[E_{\mathrm{f}i} - E_{\mathrm{q}i}] \\ \dot{E}_{\mathrm{f}i} = \dfrac{1}{T_{\mathrm{A}i}}[-E_{\mathrm{f}i} + K_{\mathrm{A}i}(\Delta U_{\mathrm{t}i} + \Delta U_{\mathrm{PSS}i})] \end{cases} \tag{1}$$

where $i = 1, 2, \ldots, n$. The above parameters of the i^{th} generator are defined in [11]. With this model, the partial linearization of the system model are presented as follows.

A. Partial Linearization of Multi-machine Power System Model

The partial linearization of the multi-machine power system model (1) is carried out here. The state variables are defined as $\boldsymbol{z} = [\boldsymbol{z}_1^\top, \ldots, \boldsymbol{z}_i^\top, \ldots, \boldsymbol{z}_n^\top]^\top$, where $\boldsymbol{z}_i = [z_{i1}, z_{i2}, z_{i3}, z_{i4}]^\top = [\Delta\delta_i \;\; \Delta\omega_i \;\; E'_{\mathrm{q}i} \;\; E_{\mathrm{f}i}]^\top$. The control variable and output variable are defined as $\boldsymbol{u} = [u_1, u_2, \ldots, u_n]^\top$ and $\boldsymbol{y} = [y_1, y_2, \ldots, y_n]^\top$, respectively, where $y_i = z_{i2}$ and $u_i = \Delta U_{\mathrm{PSS}i}$. Then the model of i^{th} synchronous generator can be denoted as

$$\begin{cases} \dot{z}_i = F_i(z) + G_i(z)\boldsymbol{u}_i \\ \boldsymbol{y}_i = H_i(z) \end{cases} \quad i = 1, 2, \ldots, n \tag{2}$$

where

$$\boldsymbol{F}_i(z) = \begin{bmatrix} F_{i1} \\ F_{i2} \\ F_{i3} \\ F_{i4} \end{bmatrix} = \begin{bmatrix} \omega_{\mathrm{B}} z_{i2} \\ \dfrac{1}{2H_i}[P_{\mathrm{m}i} - P_{\mathrm{e}i} - D_i z_{i2}] \\ \dfrac{1}{T'_{\mathrm{d}0i}}[z_{i4} - z_{i3} - (x_{\mathrm{d}i} - x'_{\mathrm{d}i})I_{\mathrm{d}i}] \\ \dfrac{1}{T_{\mathrm{A}i}}(-z_{i4} + K_{\mathrm{A}i}\Delta U_{\mathrm{t}i}) \end{bmatrix}$$

$$\boldsymbol{G}_i(z) = \begin{bmatrix} 0 & 0 & 0 & \dfrac{K_{\mathrm{A}i}}{T_{\mathrm{A}i}} \end{bmatrix}^\top \quad H_i(z) = z_{i2}.$$

Then the entire multi-machine system can be written as

$$\begin{cases} \dot{\boldsymbol{z}} = \boldsymbol{F}(\boldsymbol{z}) + \boldsymbol{G}(\boldsymbol{z})\boldsymbol{u} \\ \boldsymbol{y} = \boldsymbol{H}(\boldsymbol{z}) \end{cases} \tag{3}$$

where

$$\begin{aligned} \boldsymbol{F}(\boldsymbol{z}) &= [\boldsymbol{F}_1^\top(\boldsymbol{z}), \boldsymbol{F}_2^\top(\boldsymbol{z}), \ldots, \boldsymbol{F}_n^\top(\boldsymbol{z})]^\top \\ \boldsymbol{G}(\boldsymbol{z}) &= \mathrm{block\,diag}\,[\boldsymbol{G}_1(\boldsymbol{z}), \boldsymbol{G}_2(\boldsymbol{z}), \ldots, \boldsymbol{G}_n(\boldsymbol{z})] \\ \boldsymbol{H}(\boldsymbol{z}) &= [H_1(\boldsymbol{z}), H_2(\boldsymbol{z}), \ldots, H_n(\boldsymbol{z})]^\top. \end{aligned}$$

A nonlinear coordinate transformation is introduced as $\boldsymbol{x} = [x_{11}, x_{12}, \ldots, x_{1r}, \ldots, x_{i1}, x_{i2}, \ldots, x_{ir}, \ldots, x_{n1}, x_{n2}, \ldots, x_{nr}]^\top = \boldsymbol{T}(\boldsymbol{z}) = [H_1(\boldsymbol{z}), \mathcal{L}_F H_1(\boldsymbol{z}), \ldots, \mathcal{L}_F^{r-1} H_1(\boldsymbol{z}), \ldots, H_i(\boldsymbol{z}), \mathcal{L}_F H_i(\boldsymbol{z}), \ldots, \mathcal{L}_F^{r-1} H_i(\boldsymbol{z}), \ldots, H_n(\boldsymbol{z}), \mathcal{L}_F H_n(\boldsymbol{z}), \ldots, \mathcal{L}_F^{r-1} H_n(\boldsymbol{z})]^\top$

where r is the relative degree of ith generator model. Consequently, the multi-machine power system model is decoupled and the model of i^{th} subsystem can be written as

$$\begin{cases} \dot{x}_{i1} = x_{i2} \\ \dot{x}_{i2} = x_{i3} \\ \dot{x}_{i3} = \alpha_i(x) + \sum_{j=1}^{n} \beta_{ij}(x) u_j \\ y_i = x_{i1} \end{cases} \quad i = 1, 2, \ldots, n \tag{4}$$

where

$$\alpha_i(x) = (\mathcal{L}_F^r H_i(z))|_{z=T^{-1}(x)}$$
$$\beta_{ij}(x) = (\mathcal{L}_{G_j} \mathcal{L}_F^{r-1} H_i(z))|_{z=T^{-1}(x)}.$$

The derivatives of $H_i(z)$ are presented in Appendix A.

Considering the derivatives of active power output $P_{\text{e}i}$, the system obtained from the previous nonlinear coordination transformation can be further decoupled. On top of that, the derivatives of $P_{\text{e}i}$ can be denoted as

$$\frac{dP_{\text{e}i}}{dt} = \sum_{j=1}^{n} \left(\frac{\partial P_{\text{e}i}}{\partial z_{j3}} F_{j3} + \frac{\partial P_{\text{e}i}}{\partial z_{j1}} F_{j1} \right) = P_{\text{d}}$$

$$\frac{d^2 P_{\text{e}i}}{dt^2} = \sum_{j=1}^{n} \left(\frac{\partial P_{\text{d}}}{\partial z_{j1}} F_{j1} + \frac{\partial P_d}{\partial z_{j2}} F_{j2} + \frac{\partial P_d}{\partial z_{j3}} F_{j3} + \frac{\partial P_d}{\partial z_{j4}} F_{j4} \right) + \sum_{j=1}^{n} \frac{K_{\text{A}j}}{T_{\text{A}j}} \frac{\partial P_d}{\partial z_{j4}} u_j = \mathcal{L}_F P_d + \sum_{j=1}^{n} \frac{K_{\text{A}j}}{T_{\text{A}j}} \frac{\partial P_d}{\partial z_{j4}} u_j.$$

Meanwhile, the following can be obtained

$$\mathcal{L}_F^3 H_i(\boldsymbol{z}) = -\frac{1}{2H_i} \mathcal{L}_F P_{\text{d}} - \mathcal{L}_F \left[\frac{D_i}{2H_i} F_{i2}(\boldsymbol{z}) \right]$$
$$= -\frac{1}{2H_i} \left(\frac{d^2 P_{\text{e}i}}{dt^2} - \sum_{j=1}^{n} \frac{K_{\text{A}j}}{T_{\text{A}j}} \frac{\partial P_{\text{d}}}{\partial z_{j4}} u_j \right) - \mathcal{L}_F \left[\frac{D_i F_{i2}(\boldsymbol{z})}{2H_i} \right]$$
$$\mathcal{L}_F F_{i2}(\boldsymbol{z}) = \sum_{j=1}^{n} \left[\frac{\partial F_{i2}(\boldsymbol{z})}{\partial z_{j1}} F_{j1}(\boldsymbol{z}) + \frac{\partial F_{i2}(\boldsymbol{z})}{\partial z_{j2}} F_{j2}(\boldsymbol{z}) + \frac{\partial F_{i2}(\boldsymbol{z})}{\partial z_{j3}} F_{j3}(\boldsymbol{z}) \right]$$
$$\frac{\partial P_{\text{d}}}{\partial z_{m4}} = \frac{\partial P_{\text{e}i}}{\partial z_{m3}} \frac{1}{T'_{\text{d}0m}}.$$

Therefore, we have

$$\mathcal{L}_F^3 H_i(\boldsymbol{z}) = -\frac{1}{2H_i} \ddot{P}_{\text{e}i} - \frac{D_i}{2H_i} \mathcal{L}_F [F_{i2}(\boldsymbol{z})] - \sum_{m=1}^{n} [\mathcal{L}_{G_m} \mathcal{L}_F^2 H_i(\boldsymbol{z}) u_m]. \tag{5}$$

Hence, according to (4), it can be obtained that

$$\alpha_i(\boldsymbol{z}) = -\frac{1}{2H_i} \frac{d^2 P_{\text{e}i}}{dt^2} - \frac{D_i}{2H_i} \mathcal{L}_F [F_{i2}(\boldsymbol{z})] - \sum_{m=1}^{n} \beta_{im} u_m$$

then the system model can be written as

$$\begin{cases} \dot{x}_{i1} = x_{i2} \\ \dot{x}_{i2} = x_{i3} \\ \dot{x}_{i3} = -\frac{1}{2H_i} \left\{ \frac{d^2 P_{\text{e}i}}{dt^2} + D_i \mathcal{L}_F [F_{i2}(\boldsymbol{z})] \right\} \\ y_i = x_{i1}. \end{cases} \tag{6}$$

Meanwhile, concerning the second-order derivative of $P_{\text{e}i}$ with respect to time

$$\frac{d^2 P_{\text{e}i}}{dt^2} = 2\dot{I}_{\text{q}i} \dot{E}'_{\text{q}i} + I_{\text{q}i} \ddot{E}'_{\text{q}i} + E'_{\text{q}i} \ddot{I}_{\text{q}i} + (x_{\text{q}i} - x'_{\text{d}i}) \frac{d^2}{dt^2} (I_{\text{d}i} I_{\text{q}i})$$

x_{i3} can be rewritten as

$$\dot{x}_{i3} = f_i(x) + b_i(x) u_i \tag{7}$$

where

$$f_i(x) = \frac{-1}{2H_i} \left[2\dot{I}_{\text{q}i} \dot{E}'_{\text{q}i} + I_{\text{q}i} \ddot{E}'_{\text{q}i} + E'_{\text{q}i} \ddot{I}_{\text{q}i} + (x_{\text{q}i} - x'_{di}) \frac{d^2}{dt^2} (I_{\text{d}i} I_{\text{q}i}) \right] - \frac{D_i}{2H_i} \mathcal{L}_F [F_{i2}(\boldsymbol{z})] - \frac{I_{\text{q}i}}{2H_i T'_{\text{d}0i}} [F_{i4}(\boldsymbol{z}) - \dot{E}_{\text{q}i}]$$
$$b_i(x) = -\frac{I_{\text{q}i} K_{\text{A}i}}{2H_i T'_{\text{d}0i} T_{\text{A}i}}.$$

III. Design of the SPSS

A. Third-order BCFC

Since the relative degree of (1) is $r = 3$, a third-order BCFC is adopted based on [9]. Its feasibility assumptions can be described as follows.

$\mathbf{F}_1$: (1) can be transformed to its equivalent system written in Byrnes-Isidori normal form

$$\begin{cases} y^{(r)} = f(Y^{r-1}, z) + g(Y^{r-1}, z) u \\ \dot{z} = h(Y^{r-1}, z) \end{cases} \tag{8}$$

where $Y^{r-1} := (y, \dot{y}, \ldots, y^{(r-1)})$, y is the system output, r is the relative degree of y with respect to u, z is the zero state vector of system, f, g, h are locally Lipschitz continuous, and g is positive. It is assumed that the zero state of the system is stable.

$\mathbf{F}_2$: $y_{\text{ref}} \in \mathcal{C}^{r-1}$ and $y_{\text{ref}}^{(r-1)}$ is absolutely continuous with right-continuous derivative.

The switching logic of a third-order bang-bang constant funnel controller can be given as

$$\begin{aligned} & q_1(t) = \mathcal{G}(e(t), \varphi_0^+ - \varepsilon_0^+, \varphi_0^- + \varepsilon_0^-, q_1(t-)) \\ & q_1(0-) = q_1^0 \in \{\text{true}, \text{false}\} \\ & q_2(t) = \begin{cases} \mathcal{G}(\dot{e}(t), -\lambda_1^- - \varepsilon_1^+, \varphi_1^- + \varepsilon_1^-, q_2(t-)), \\ \text{if } q_1(t) = \text{true} \\ \mathcal{G}(\dot{e}(t), \varphi_1^+ - \varepsilon_1^+, \lambda_1^+ + \varepsilon_1^-, q_2(t-)), \\ \text{if } q_1(t) = \text{false} \end{cases} \\ & q_2(0-) = q_2^0 \in \{\text{true}, \text{false}\} \\ & q(t) = \begin{cases} \mathcal{G}(\ddot{e}(t), -\lambda_2^- - \varepsilon_2^+, \varphi_2^-(t) + \varepsilon_2^-, q(t-)), \\ \text{if } q_2(t) = \text{true} \\ \mathcal{G}(\ddot{e}(t), \varphi_2^+ - \varepsilon_2^+, \lambda_2^+ + \varepsilon_2^-, q(t-)), \\ \text{if } q_2(t) = \text{false} \end{cases} \\ & q(0-) = q^0 \in \{\text{true}, \text{false}\} \end{aligned} \tag{9}$$

where $q(t), q_1(t), q_2(t) \in \{\text{true}, \text{false}\}$, $q(t)$ is the output of the switching logic, $\mathcal{G}(e(t), \overline{e}, \underline{e}, q(t-)) := [e(t) \geq \overline{e} \vee (e(t) > \underline{e} \wedge q_{\text{old}})]$, $e(t)$ is the tracking error of system output, $\overline{e}(\cdot)$ is

the upper trigger of a switch event, $\underline{e}(\cdot)$ is the lower trigger of a switch event, $q(t-) := \lim_{\varepsilon\to 0} q(t-\varepsilon)$, $\varphi_i^{\pm}$, $\varepsilon_i^{\pm}$ and $\lambda_j^{\pm}$ are constant values used to define funnel $\mathcal{F}_i (i = 0, 1, 2; j = 1, 2)$. The control law of the BCFC can be simply given as

$$u(t) = \begin{cases} U^-, & \text{if } q(t) = \text{true}, \\ U^+, & \text{if } q(t) = \text{false}. \end{cases}$$

The working mechanism of the third-order BCFC is shown in Fig. 1. The system output tracking error and its first- and second-order derivative can be regulated within the pre-specified error funnel $\mathcal{F}_i (i = 0, 1, 2)$ through the bang-bang control signal $u(t)$.

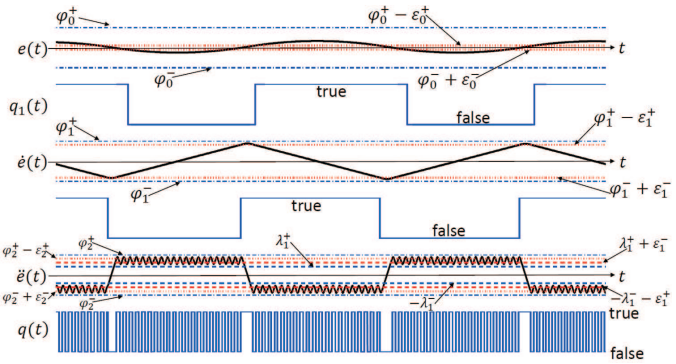

Fig. 1. Working mechanism of the third-order bang-bang constant funnel controller.

B. Design of the Third-order BPSS

Based on (7) and the BCFC, a third-order BPSS is designed here. The switching logic of the second-order BEC and BG has been described in Section III-A. The funnel parameters of the BEC and BG should be chosen satisfying $\varphi_0^+ - \varepsilon_0^+ > \varphi_0^- + \varepsilon_0^-$ and $\varphi_i^+ - \varepsilon_i^+ > \varepsilon_i^- + \lambda_i^+$, $\varphi_i^- + \varepsilon_i^- < -\lambda_i^- - \varepsilon_i^+ (i = 1, 2)$.

With respect to $\mathbf{F}_1$, the multi-machine power system model has been transformed into Byrnes-Isidori form in Section II-A and its zero dynamics can be easily verified to be stable. Concerning the positiveness of $b_i(x)$, since $P_{ei} = E'_{qi} I_{qi}$ and $E'_{qi} > 0$ and $P_{ei} > 0$, we have $I_{qi} > 0$. Considering $b_i(x) = -(I_{qi} K_{Ai})/(2H_i T'_{d0i} T_{Ai})$, it can be obtained that $b_i(x) < 0$. In order to satisfy the positiveness of $b_i(x)$, (7) is rewritten as $\dot{x}_{i3} = f_i(x) + b'_i(x) u'_i$, where $u'_i = -u_i, b'_i(x) = -b_i(x)$. Hence, we have $b'_i(x) > 0$. Correspondingly, $U^{+\prime} = U^- > 0$, and $U^{-\prime} = U^+ < 0$ hold. Therefore, the control law of the BPSS is simply given by

$$u_i(t) = \begin{cases} u^+_{\text{PSS}i} & (\text{if } q(t) = \text{true}) \\ u^-_{\text{PSS}i} & (\text{if } q(t) = \text{false}). \end{cases} \tag{10}$$

C. State-dependent Switching Strategy of the SPSS

The SPSS is designed to switch between the BPSS and the CPSS to damp the oscillations of rotor angle based on a state-dependent switching strategy $\mathcal{T}$. The overall schematic of the SPSS is illustrated in Fig. 2. Assume that the maxima sequence of the absolute output tracking error $|e_i(t)| = |y_i(t) - y_{i\text{ref}}(t)|$ is $\Gamma_i(t) = \{\Gamma_{i1}, \Gamma_{i2}, \ldots, \Gamma_{ij}\}$ in the case that $e_i(t)$ is oscillating after disturbances occur in the power system, and Γ_{is} $(s \in \{1, 2, \ldots, j\})$ is the maximum of the sequence $\Gamma_i(t)$. The switching strategy is that the SPSS switches from CPSS to BPSS if $\mathcal{T}_1$ is satisfied and switches from BPSS to CPSS if $\mathcal{T}_2$ is satisfied, where $\mathcal{T}_1$ and $\mathcal{T}_2$ are illustrated as follows,

$\mathcal{T}_1$: $\{|e_i(t)| \geq \varpi\}$,

$\mathcal{T}_2$: {The switching frequency of BPSS reaches its maximum} $\vee$ $\{\{(\Gamma_{is} - \Gamma_{ij})/\Gamma_{is} \geq \tau\} \wedge \{e_i(t)$ converges within $[(\varphi_0^- + \varepsilon_0^-), (\varphi_0^+ - \varepsilon_0^+)]\}\}$,

where ϖ, τ are design parameters of the SPSS installed on ith generator. ϖ is the value of output tracking error that triggers the BPSS, and it can be determined according to the desired oscillation magnitude to be damped. τ is selected referring to the desired damping rate of the magnitude of the system output tracking error.

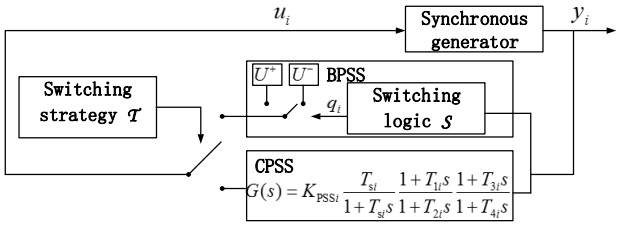

Fig. 2. Schematic of the SPSS.

IV. Closed-loop Stability

The primary objective of the PSS is to generate an auxiliary signal to provide additional damping to the oscillations of rotor speed. Therefore, the kinetic energy of a synchronous generator is considered as its energy function for the closed-loop stability analysis of the multi-machine power system. Then the energy function of the multi-machine power system can be denoted as

$$V = \frac{1}{2} \sum_{i=1}^{n} (2H_i \Delta\omega_i^2) = \frac{1}{2} \sum_{i=1}^{n} (2H_i x_{i1}^2). \tag{11}$$

Assume that SPSSs are installed on the first m synchronous generators. For the last $n - m$ generators only installed with CPSSs, their energy function can be written as

$$V_{m-n} = \frac{1}{2} \sum_{i=m+1}^{n} (2H_i x_{i1}^2). \tag{12}$$

Then its difference can be written as

$$dV_{m-n} = \sum_{i=m+1}^{n} (2H_i x_{i1} dx_{i1}) \tag{13}$$

where $d\Theta = [\Theta(i+1) - \Theta(i)]$, $\Theta(i)$ is the value of $\Theta(t)$ at $t = t_i$ and $2H_i dx_{i1} = -dP_{ei}$ which is obtained based on the assumption of $D_i = 0$. Due to that $P_{ei} = \omega_i T_{ei}$ and $\omega_i \approx 1$ if the operation point of the power system is around the equilibrium point, we have $dP_{ei} = dT_{ei}$. Specifically, the CPSS is usually designed to produce an additional electromechanical torque that is in the same phase with that of $\Delta\omega_i$ [12]; in other words, $dT_{ei} = D_{ei} \Delta\omega_i = D_{ei} x_{i1}$ holds, where D_{ei} is

determined by the parameters of the CPSS, which ensures that $D_{ei} > 0$. Hence, (12) can be rewritten as

$$dV_{m-n} = -\sum_{i=m+1}^{n} D_{ei} x_{i1}^2. \tag{14}$$

On condition that the operation point of the power system leaves the normal stable point and $|x_{i1}| > 0$, then $dV_{m-n} < 0$ holds. Therefore, V_{m-n} serves as a stable energy function of the synchronous generators installed with CPSS.

With respect to generators implemented with the SPSS, we assume that a negative disturbance occurs at $t = t_0$. The BPSS is switched on first to regulate the tracking error of rotor speed and its derivatives back into the pre-specified error funnels. Fig. 3 is presented to support the following discussion, in which $e^{(0)}(t) = x_{i1} = \Delta\omega_i (i = 1, 2, \ldots, m)$. Assume that there exists a minimal t_4 such that $e^{(1)}(t_4) \geq 0$ and minimal t_3 such that $e^{(0)}(t_3) = \varphi_0^+ - \varepsilon_0^+$. In the following, we will show that $e^{(0)}(t)$ is monotonically increasing on the interval $[t_4, t_3)$.

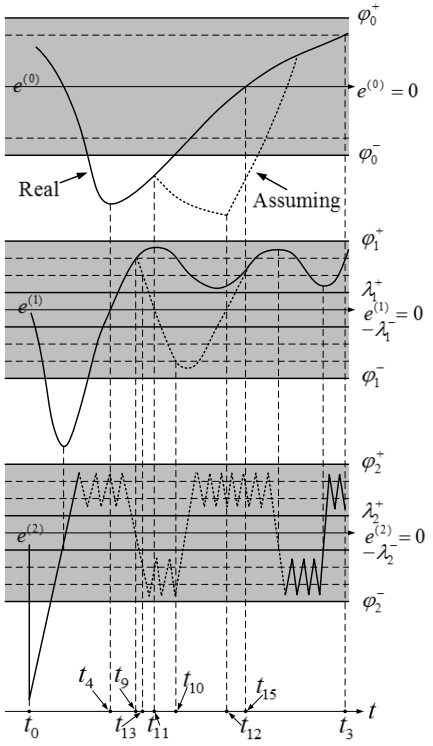

Fig. 3. Illustration showing $e^{(0)}(t)$ is monotonically increasing on interval $[t_4, t_3)$.

Seeking a contradiction, assume that there exists an interval $[t_{11}, t_{12}] \in [t_4, t_3)$ on which $e^{(0)}(t)$ is decreasing. Concerning the switching logic of q_2, there exists a minimal $t_9 \in (t_4, t_{11})$ such that $e^{(1)}(t_9) = \varphi_1^+ - \varepsilon_1^+$. Hence, $q_2(t_9) = \text{true}$ and $q_2(t) = \text{true}$ hold on the interval $[t_9, t_{10})$ and we assume $e^{(1)}(t)$ hits $\varphi_1^- + \varepsilon_1^-$ at $t = t_{10}$. However, considering the switching logic of q_1, $q_1 = \text{false}$ holds on interval $[t_4, t_3)$. Concerning $q_2(t) = \mathcal{G}(e^{(1)}(t), \varphi_1^+ - \varepsilon_1^+, \lambda_1^+ + \varepsilon_1^-, q_2(t-))$ (if $q_1(t) = \text{false}$), $q_2(t)$ will turn false when $e^{(1)}(t)$ hits $\lambda_1^+ + \varepsilon_1^-$. Hence, $q_2(t) = \text{false}$ holds on the interval $t \in [t_{13}, t_{10})$, whence the contradiction is obtained.

From the above analysis and the illustration of Fig. 3, it shows that x_{i1} will converge into the error funnels monotonically from t_4 after the impulsive disturbance occurs in the system. Therefore, the energy function of the generators installed with SPSS is monotonically decreasing and the rotor speed of these generators converges into the invariant region defined by the error funnels on the interval $[t_4, t_{15}]$. Hence, $V_{1-m} = \frac{1}{2}\sum_{i=1}^{m}(2H_i x_{i1}^2)$ will decrease into the invariant region defined by the error funnels eventually. In other words,

$$dV_{1-m} = \sum_{i=1}^{m}(2H_i x_{i1} dx_{i1}) < 0 \tag{15}$$

holds on the interval $[t_4, t_{15}]$. Within the error funnel $\mathcal{F}_0$, the CPSS will be switched on if the switching condition of switching the BPSS to the CPSS is satisfied. Then the difference of the energy function of the generators installed with the SPSS can be denoted as

$$dV_{1-m} = -\sum_{i=1}^{m} D_{ei} x_{i1}^2 \leq 0. \tag{16}$$

Therefore, we have shown that the energy function of n generators will converge to zero after an external disturbance occurs in the power system. The trajectories of the energy functions of the generators installed with the CPSS and SPSS respectively are illustrated in Fig. 4.

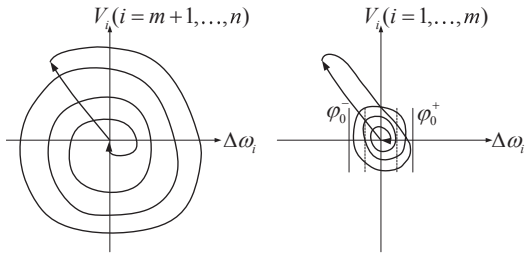

Fig. 4. Illustration of the trajectories of the energy functions of generators installed with the CPSSs and the SPSSs, respectively.

V. Simulation Studies

To verify the oscillation damping performance of the SPSS, simulation studies are carried out in a 4-generator 11-bus power system and the IEEE 16-generator 68-bus power system, respectively. The CPSSs studied in this section are designed based on [13], [14]. These techniques account for multiple operation points and operation regimes in order to ensure PSS robustness in terms of damping. They are so effective that, with minor variations, they remain the state of the art currently employed in industry to date.

A. Mechanical Power Change Occurs in a 4-generator 11-bus Power System

A 4-generator 11-bus power system is used here for case studies, whose structure is presented in Fig. 5. Parameters of synchronous generators, transmission lines and loads are presented in [15]. The simplified first-order excitation controller presented in Section II is installed in every generator, and the parameters of the excitation controller are given in Table I.

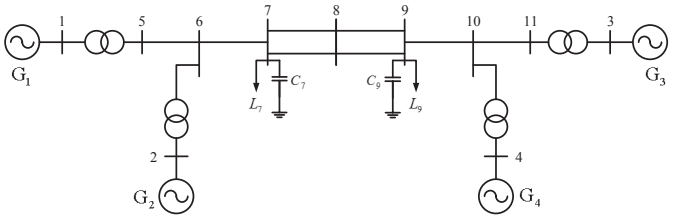

Fig. 5. Structure of the 4-generator 11-bus power system.

TABLE I
PARAMETERS OF CPSS AND EXCITATION CONTROLLER OF THE 4-GENERATOR 11-BUS POWER SYSTEM

Parm.[a]	Value	Parm.	Value	Parm.	Value
T_{si}	7.5	T_{1i}	0.08	T_{2i}	0.015
T_{3i}	0.08	T_{4i}	0.015	$K_{\mathrm{PSS}i}$	20
$u^{+}_{\mathrm{PSS}i}$	0.1	$u^{-}_{\mathrm{PSS}i}$	-0.1	$T_{\mathrm{A}i}$	0.01
$K_{\mathrm{A}i}$	20	$E^{+}_{\mathrm{f}j}$	3	$E^{-}_{\mathrm{f}j}$	-3

a. Parm. represents parameter.
$i = 3, 4$, $j = 1, 2, 3, 4$
$+$ denotes the upper limit of the variable.
$-$ denotes its lower limit.

In order to evaluate the damping performance of the SPSS, generator 3 and generator 4 are installed with the SPSS, and the parameters of the SPSS are given in Appendix B. The other generators of the system do not have a PSS installed. The parameters of the CPSS of the SPSS implemented on generator 3 and generator 4 are presented in Table I. The simulation step length is set as $h = 0.01$ s.

The mechanical power input of generator 1 has a 0.1 p.u. increase at $t = 1$ s. The dynamics of the power system is presented in Fig. 6. According to Fig. 6(a) and Fig. 6(b), less inter-machine oscillations can be found in the power system having the SPSS installed. The power system only having the CPSS implemented even goes unstable. From Fig. 6(c) and Fig. 6(d), generator 3 and generator 4 controlled by the SPSS respectively show less fluctuation in their rotor speed. This is due to the control input generated by the SPSS, which is presented in Fig. 6(e) and Fig. 6(f). It can be observed that the SPSS utilizes the maximum and the minimum of the output of the PSS and is able to provide proper switching of the control inputs. Consequently, the SPSS makes use of the utmost control energy of the PSS and enhances the small-signal stability of the 4-generator 11-bus power system.

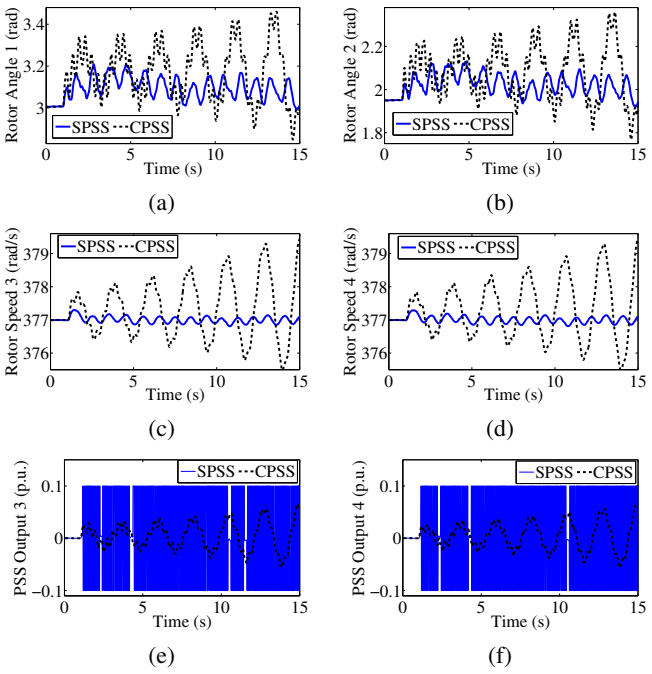

Fig. 6. Mechanical power change occurs in generator 1 in the 4-generator 11-bus power system. (a) Rotor angle deviation between generator 1 and generator 3. (b) Rotor angle deviation between generator 2 and generator 3. (c) Rotor speed of generator 3. (d) Rotor speed of generator 4. (e) Control input of the PSS of generator 3. (f) Control input of the PSS of generator 4.

Moreover, it should be mentioned that the inputs of the SPSS is generated by magnifying the rotor speed deviation of generators in rad/s, i.e., $200\Delta\omega$. In this way, the same set of control parameters of the SPSS are adopted in this paper, and this does not influence the performance of the SPSS.

B. Load Change Occurs in the IEEE 16-generator 68-bus Power System

In order to verify the small-signal oscillation damping performance of the SPSS in a large-scale power system, the IEEE 16-generator 68-bus power system is used here, whose layout is illustrated in Fig. 7. The parameters of synchronous generators, transmission lines, and loads are given in [16]. A simplified first-order excitation controller, which has been given in Section II, is applied in all synchronous generators. Generators 1, 10, 11, 12, 13 and 16 are implemented with a PSS, respectively, and the SPSS is installed on generator 1, 10, and 11, respectively. The parameters of the SPSS are presented in Appendix B. Then the parameters of the CPSS and excitation controller are illustrated in Appendix C. The simulation step length is set as $h = 0.01$ s.

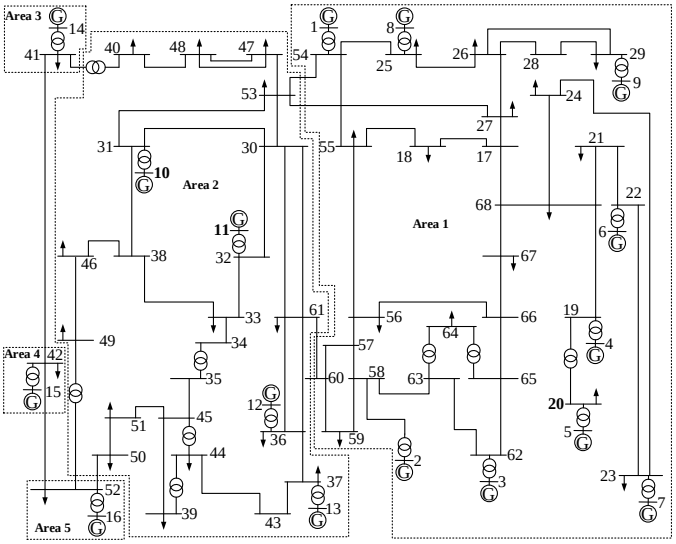

Fig. 7. The layout of the IEEE 16-generator 68-bus power system.

In this case, a 0.5 p.u. load decrease occurs on bus 20 at $t = 1$ s in the IEEE 16-generator 68-bus power system, and the load is recovered at $t = 1.2$ s. The load decrease results in a 0.03 Hz frequency increase in the power system only having the CPSS installed, while it only leads to a 0.01 Hz

frequency increase in the system having the SPSS installed as depicted in Fig. 8(j). The rotor angle deviation and the rotor speed of generator 1, 10, and 11 are illustrated in Fig. 8(a)–(f), respectively. It can be seen that the rotor angle deviation and the rotor speed of the generators having the SPSS installed present less oscillations than those of the generators having only the CPSS installed. Although the BPSS of generator 11 is not switched on during this process as depicted in Fig. 8(i), the control effort of the SPSS of generator 1 and generator 10 is able to stabilize the power system to its original operation point. Just as presented in Fig. 8(g) and 8(h), the SPSSs of generator 1 and generator 10 are able to provide proper switching of control inputs and they utilize the maximum control energy to damp the oscillations of rotor speed. Owning to the above, the frequency of the power system having the SPSS installed shows less deviation and less fluctuation than that of the power system only having the CPSS implemented as illustrated in Fig. 8(j).

C. Load Trip Occurs in the IEEE 16-generator 68-bus Power System

In order to evaluate the influence of the SPSS with respect to the transient stability of power systems, a new case, in which load trip of bus 20 occurs in the IEEE 16-generator 68-bus power system, is studied here. The configuration of the power system is the same as that studied in Section V-B. Specifically, the load of bus 20 trips at $t = 1$ s and it recovers at $t = 1.05$ s. This leads to a frequency deviation of 0.14 Hz in the power system having only the CPSS installed. By contrast, the frequency deviation of the power system having the SPSS installed is only 0.04 Hz as depicted in Fig. 9(j).

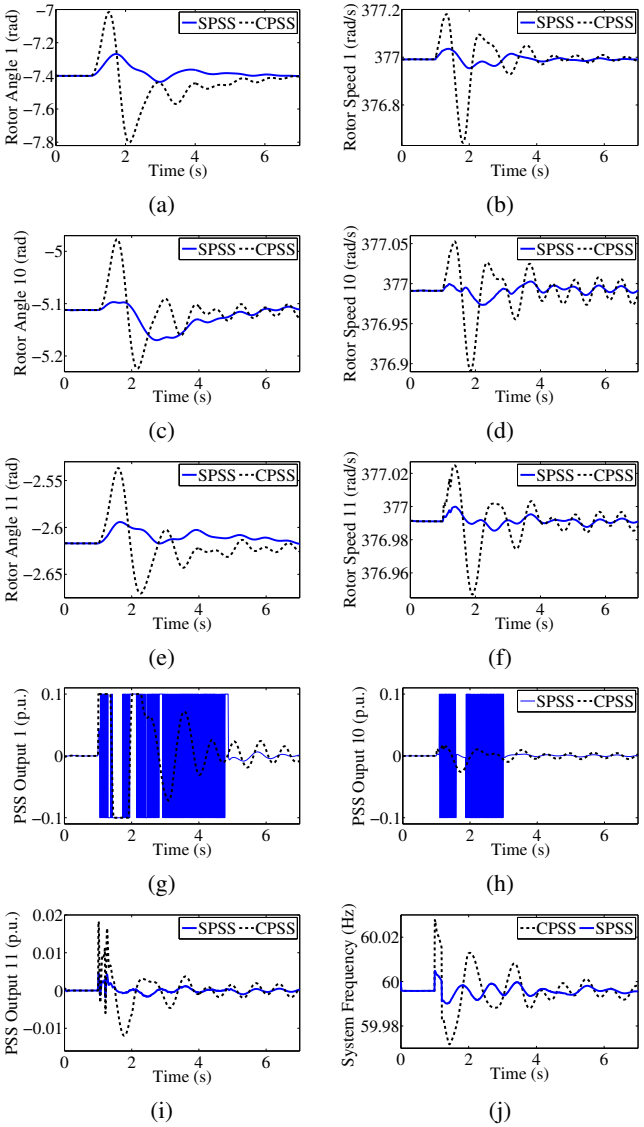

Fig. 8. Load change occurs in the IEEE 16-generator 68-bus power system. (a) Rotor angle of generator 1. (b) Rotor speed of generator 1. (c) Rotor angle of generator 10. (d) Rotor speed of generator 10. (e) Rotor angle of generator 11. (f) Rotor speed of generator 11. (g) Control input of the PSS of generator 1. (h) Control input of the PSS of generator 10. (i) Control input of the PSS of generator 11. (j) Frequency response of the power system.

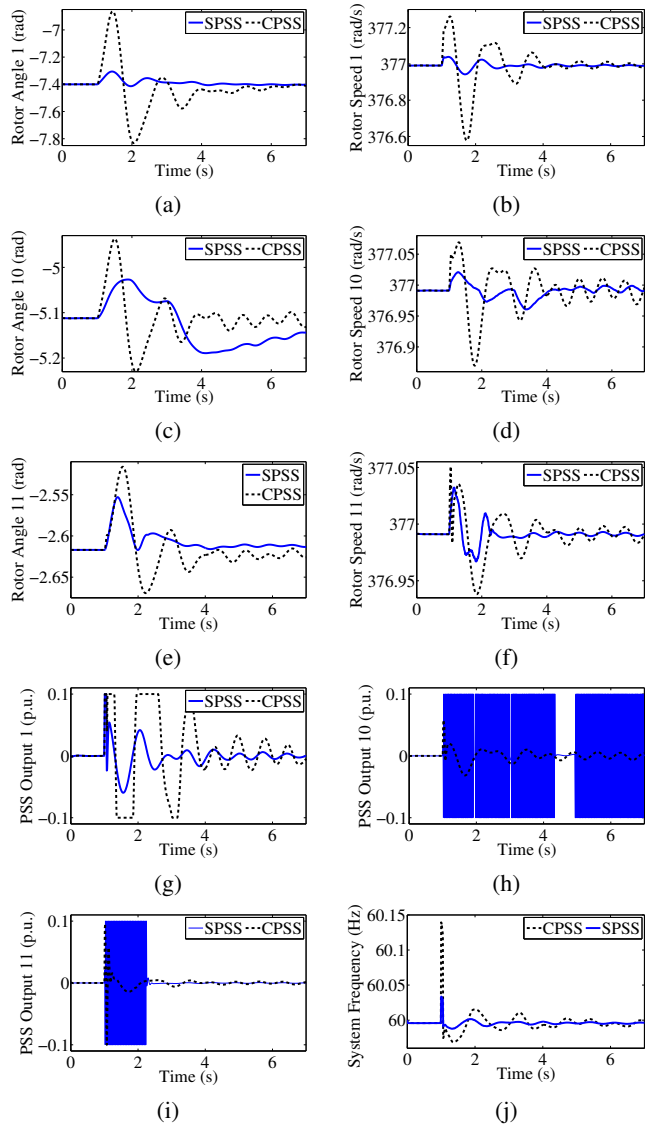

Fig. 9. Load trip occurs in the IEEE 16-generator 68-bus power system. (a) Rotor angle of generator 1. (b) Rotor speed of generator 1. (c) Rotor angle of generator 10. (d) Rotor speed of generator 10. (e) Rotor angle of generator 11. (f) Rotor speed of generator 11. (g) Control input of the PSS of generator 1. (h) Control input of the PSS of generator 10. (i) Control input of the PSS of generator 11. (j) Frequency response of the power system.

The rotor angle deviation and rotor speed of generator 1, generator 10 and generator 11 are presented in Fig. 9(a)–(f). It can be observed that the generators having the SPSS installed present stronger damping of the oscillations than the ones having only the CPSS installed. Moreover, the control inputs generated by the PSSs are illustrated in Fig. 9(g)–(i). The BPSS of generator 1 is not switched on in this case, and the damping performance of the power system having the SPSS installed is mainly achieved by the effort of the SPSS installed on generator 10 and generator 11, respectively. Then less frequency deviation can be found in the power system having the SPSS implemented as depicted in Fig. 9(j).

VI. Conclusion

This paper has proposed a coordinated SPSS to enhance the stability of multi-machine power systems.

The design of the BPSS does not rely on an accurate system model and only the knowledge of relative degree of the system is required. The presented switching strategy of the SPSS has twofold merits. It utilizes the time-optimum characteristic of the BPSS and, at the same time, makes full use of the damping ability of the CPSS.

According to the simulation results, the rotor angle deviation and the rotor speed of the generators having the SPSS installed present less oscillations than those of the generators having only the CPSS implemented in the cases where small disturbances occur in the multi-machine power system studied in Section V-A and Section V-B. It reveals that the SPSS is able to provide stronger damping ability to the small-signal oscillations than the CPSS. This is because the SPSS has fully utilized its switching function and provided accurate switching time of the PSSs. Moreover, the BPSS can utilize the largest control energy of the PSS to offer the utmost damping with respect to the oscillations of rotor speed. In the case that mechanical power change occurs in a 4-generator 11-bus power system, the SPSS has prevented the power system from going unstable.

The SPSS helps to improve the transient stability of multi-machine power systems as well. Referring to the case that load trip occurs in the IEEE 16-generator 68-bus power system, the system having the SPSS installed has presented less frequency deviation and less oscillations in the rotor angle deviation and the rotor speed of generators. With the combined effort of the SPSS and the exciters, the power system having the SPSS installed has shown stronger transient stability than that having only the CPSS implemented.

Although the SPSSs are installed locally, they can coordinate with the SPSSs installed on different generators. This can be observed from the simulated results of the relative rotor angle between different generators studied in Section V-A. The interacted dynamics of generators can be cancelled with the switching of control inputs.

Moreover, the same set of SPSS parameters are used in the three cases presented in Section V. Thus the robustness of the SPSS, with respect to the change of power system operation conditions, is verified.

Appendix A
Derivatives of Output Variable

$$\mathcal{L}_F H_i(\boldsymbol{z}) = \Delta\dot{\omega}_i$$

$$\mathcal{L}_F^2 H_i(\boldsymbol{z}) = -\frac{1}{2H_i}\sum_{j=1}^{n}\left[\frac{\partial P_{ei}}{\partial z_{j1}}F_{j1}(\boldsymbol{z}) + \frac{\partial P_{ei}}{\partial z_{j3}}F_{j3}(\boldsymbol{z})\right] - \frac{D_i}{2H_i}F_{i2}(\boldsymbol{z})$$

$$\mathcal{L}_F^3 H_i(\boldsymbol{z}) = -\frac{1}{2H_i}\sum_{m=1}^{n}F_{m1}(\boldsymbol{z})$$
$$\left\{\sum_{j=1}^{n}\left[\frac{\partial P_{ei}}{\partial z_{j1}\partial z_{m1}}F_{j1}(\boldsymbol{z}) + \frac{\partial P_{ei}}{\partial z_{j3}\partial z_{m1}}F_{j3}(\boldsymbol{z}) + \frac{\partial P_{ei}}{\partial z_{j3}}\frac{\partial F_{j3}(\boldsymbol{z})}{\partial z_{m1}}\right]\right\} - \frac{D_i}{2H_i}\sum_{m=1}^{n}\left[\frac{\partial F_{i2}(\boldsymbol{z})}{\partial z_{m1}}F_{m1}(\boldsymbol{z})\right]$$
$$- \frac{\omega_{\mathrm{B}}}{2H_i}\sum_{m=1,m\neq i}^{n}\left[\frac{\partial P_{ei}}{\partial z_{m1}}F_{m2}(\boldsymbol{z})\right]$$
$$- \left[-\frac{\omega_{\mathrm{B}}}{2H_i}\frac{\partial P_{ei}}{\partial z_{i1}} + \left(\frac{D_i}{2H_i}\right)^2\right]F_{i2}(\boldsymbol{z}) - \frac{1}{2H_i}\sum_{m=1}^{n}F_{m3}(\boldsymbol{z})$$
$$\left\{\sum_{j=1}^{n}\left[\frac{\partial P_{ei}}{\partial z_{j1}\partial z_{m3}}F_{j1}(\boldsymbol{z}) + \frac{\partial P_{ei}}{\partial z_{j3}\partial z_{m3}}F_{j3}(\boldsymbol{z}) + \frac{\partial P_{ei}}{\partial z_{j3}}\frac{\partial F_{j3}(\boldsymbol{z})}{\partial z_{m3}}\right]\right\} - \frac{D_i}{2H_i}\sum_{m=1}^{n}\left[\frac{\partial F_{i2}(\boldsymbol{z})}{\partial z_{m3}}F_{m3}(\boldsymbol{z})\right]$$
$$- \frac{1}{2H_i}\sum_{m=1}^{n}\left[\frac{1}{T'_{\mathrm{d}0m}}\frac{\partial P_{ei}}{\partial z_{m3}}F_{m4}(\boldsymbol{z})\right]$$

$$\mathcal{L}_{G_m}\mathcal{L}_F^1 H_i(\boldsymbol{z}) = 0$$

$$\mathcal{L}_{G_m}\mathcal{L}_F^2 H_i(\boldsymbol{z}) = -\frac{1}{2H_i T'_{\mathrm{d}0m}}\frac{K_{\mathrm{A}m}}{T_{\mathrm{A}m}}\frac{\partial P_{ei}}{\partial z_{m3}}.$$

Appendix B
Parameters of the SPSS

Parm.[a]	Value	Parm.	Value	Parm.	Value
φ_0^+	3	φ_0^-	-3	φ_1^+	8
φ_1^-	-8	φ_2^+	100	φ_2^-	-100
ε_0^+	2.95	ε_0^-	2.95	ε_1^+	0.5
ε_1^-	0.5	ε_2^+	5	ε_2^-	5
λ_1^+	6.95	λ_1^-	6.95	λ_2^+	16.95
λ_2^-	16.95	ϖ	2	τ	0.8
U^+	0.1	U^-	-0.1		

a. Parm. represents parameter.

Appendix C
Parameters of CPSS and Exciters

Parm.[a]	Value	Parm.	Value	Parm.	Value
T_{si}	7.5	T_{1i}	0.08	T_{2i}	0.015
T_{3i}	0.08	T_{4i}	0.015	$K_{\mathrm{PSS}i}$	50
$u_{\mathrm{PSS}i}^+$	0.1	$u_{\mathrm{PSS}i}^-$	-0.1	$T_{\mathrm{A}i}$	0.01
$K_{\mathrm{A}i}$	30	$E_{\mathrm{f}i}^+$	3	$E_{\mathrm{f}i}^-$	-3

a. Parm. represents parameter.
$+$ denotes the upper limit.
$-$ denotes the lower limit of the variable.

REFERENCES

[1] R. Grondin, I. Kamwa, L. Soulieres, J. Potvin, and R. Champagne, "An approach to PSS design for transient stability improvement through supplementary damping of the common low-frequency," *IEEE Transactions on Power Systems*, vol. 8, no. 3, pp. 954–963, Aug. 1993.

[2] N. Martins and L. T. Lima, "Determination of suitable locations for power system stabilizers and static var compensators for damping electromechanical oscillations in large scale power systems," *IEEE Transactions on Power Systems*, vol. 5, no. 4, pp. 1455–1469, Nov. 1990.

[3] S.-K. Wang, "A novel objective function and algorithm for optimal PSS parameter design in a multi-machine power system," *IEEE Transactions on Power Systems*, vol. 28, no. 1, pp. 522–531, Feb. 2013.

[4] C. T. Tse and S. K. Tso, "Refinement of conventional PSS design in multimachine system by modal analysis," *IEEE Transactions on Power Systems*, vol. 8, no. 2, pp. 598–605, May 1993.

[5] J. Zhang, C. Chung, and Y. Han, "A novel modal decomposition control and its application to PSS design for damping interarea oscillations in power systems," *IEEE Transactions on Power Systems*, vol. 27, no. 4, pp. 2015–2025, Nov. 2012.

[6] S. Yuan and D. Z. Fang, "Robust PSS parameters design using a trajectory sensitivity approach," *IEEE Transactions on Power Systems*, vol. 24, no. 2, pp. 1011–1018, May 2009.

[7] C. Chung, K. Wang, C. Tse, and R. Niu, "Power-system stabilizer PSS design by probabilistic sensitivity indexes PSIs," *IEEE Transactions on Power Systems*, vol. 17, no. 3, pp. 688–693, Aug. 2002.

[8] D. Trudnowski, D. Pierre, J. Smith, and R. Adapa, "Coordination of multiple adaptive PSS units using a decentralized control scheme," *IEEE Transactions on Power Systems*, vol. 7, no. 1, pp. 294–300, Feb. 1992.

[9] D. Liberzon and S. Trenn, "The bang-bang funnel controller for uncertain nonlinear systems with arbitrary relative degree," *IEEE Transactions on Automatic Control*, vol. 58, no. 12, pp. 3126–3141, Dec. 2013.

[10] H. T. Kang, Y. Liu, Q. H. Wu, and X. X. Zhou, "Switching excitation controller for enhancement of transient stability of multi-machine power systems," *CSEE Journal of Power and Energy Systems*, vol. 1, no. 3, pp. 86–94, Sep. 2015.

[11] L. Jiang, Q. H. Wu, and J. Y. Wen, "Decentralized nonlinear adaptive control for multimachine power systems via high-gain perturbation observer," *IEEE Transactions on Circuits and Systems I: Regular Papers*, vol. 51, no. 10, pp. 2052–2059, Oct. 2004.

[12] Q. Lu, Y. Sun, and S. Mei, *Nonlinear Control Systems and Power System Dynamics*. Springer, 2001.

[13] E. Larsen and D. Swann, "Applying power system stabilizers part I: General concepts," *IEEE Transactions on Power Apparatus and System*, vol. PAS-100, no. 6, pp. 3017–3024, Jun. 1981.

[14] E. Larsen and D. Swann, "Applying power system stabilizers part II: Performance objectives and tuning concepts," *IEEE Transactions on Power Apparatus and System*, no. 6, pp. 3025–3033, Jun. 1981.

[15] P. Kundur, *Power System Stability and Control*. New York: McGraw-hill, 1994.

[16] R. SadikoviC, "Use of facts devices for power flow control and damping of oscillations in power systems," Ph.D. dissertation, Swiss Fedral Institute of Technology Zurich, 2006.

Yang Liu obtained a B.E. degree in electrical engineering from South China University of Technology (SCUT), Guangzhou, China, in 2012. He is currently pursing the Ph.D degree in the same area in SCUT. His research interests include the area of power system stability control and power quality evaluation.

Qinghua Wu (M'91, SM'97, F'11) obtained a Ph.D. degree in electrical engineering from The Queens University of Belfast (QUB), U.K. in 1987. He worked as a Research Fellow and subsequently a Senior Research Fellow in QUB from 1987 to 1991. He joined the Department of Mathematical Sciences, Loughborough University, U.K. in 1991, as a Lecturer, subsequently he was appointed Senior Lecturer. In 1995, he joined The University of Liverpool, U.K. to take up the Chair of Electrical Engineering in the Department of Electrical Engineering and Electronics. Now he is with the School of Electric Power Engineering, South China University of Technology, China, as a Distinguished Professor and the Director of Energy Research Institute of the University. Professor Wu has published more than 440 technical publications, including 220 journal papers, 20 book chapters and 3 research monographs published by Springer. He is a Fellow of IEEE, Fellow of IET, Chartered Engineer and Fellow of InstMC. His research interests include nonlinear adaptive control, mathematical morphology, evolutionary computation, power quality and power system control and operation. He has received a National Semiconductor Advanced Technology Award, National Semiconductor Corporation, USA; Remuneration Award to an exceptional merit and performance, Science and Engineering Research Council, UK; Donald Julius Groen Prize for the best paper published in Journal of Systems and Control Engineering. His research interests include nonlinear adaptive control, mathematical morphology, evolutionary computation, power quality and power system control and operation.

Haotian Kang obtained a B.Sc degree in mathematics and applied mathematics from South China University of Technology (SCUT), Guangzhou, China. He is currently pursuing the M.Sc. degree in electrical engineering in SCUT. His research interest is within the area of power system stability control.

Xiaoxin Zhou (F'95) graduated from Tsinghua University, China, in 1965. He is a member of Chinese Academy of Sciences (CAS), a Fellow of IEEE and Academician of Chinese Academy of Sciences. Currently he also serves as the Honorary President of China Electric Power Research Institute (CEPRI), Executive Director of China Society of Electrical Engineering (CSEE), Director of the Study Committee, and the Executive Director of China Electrotechnical Society (CES).

Professor Zhou has devoted himself to research on power system analysis and computation methods for decades. He has led his research group and successfully developed the Power System Analysis Software Package (PSASP), the first large-sale power system analysis software in China, which has been widely applied in the Chinese power utilities. Since the 1990s, he has committed to research on power electronics, digital simulation technology, and power system security and stability monitoring and control theory. Additionally, he has managed a national basic research program, "Research on the fundamental theory of improving operation reliability of the large-scale interconnected power systems," and serves as the chief scientist. Professor Zhou won the top-grade national science and technology progress award for three times in 1985, 2008, and 2009, respectively. He also won the IEEE PES Nari Hingorani FACTS Award in 2008 and the Prize of Ho Leung Ho Lee Foundation for Scientific and Technological Progress in 2009. His main research interests include power system analysis and control, power system digital simulation, flexible AC transmission system (FACTS).